Nuclear Physics B251[FS13](1985)127-140

THE PHASES OF THE O(3) σ-MODEL FOR IMAGINARY ϑ

Gyan BHANOT and Francois DAVID*

The Institute for Advanced Study, Princeton, New Jersey 08540, USA

Received 5 July 1984

The lattice O(3) σ-model in two dimensions is studied for imaginary values of the vacuum angle ϑ ($\vartheta = i\vartheta_i$) and positive β by numerical simulation. We find that the theory exhibits a line of first-order transitions starting at $\beta = \infty$, $\vartheta = i\infty$ which ends in the (β, ϑ_i) plane in a critical endpoint. This line separates a gas phase from a liquid-like phase of topological excitations. We illustrate the physics of the phase transitions with two simple models. We also study the effect of increasing the action of small sized instantons.

1. Introduction

The vacuum angle ϑ plays an important role in the dynamics of two-dimensional spin models and four-dimensional gauge theories. Following recent developments [1–3], it is now possible to study these topological effects in the nonperturbative framework of lattice theories. In this paper we present a numerical study of the two-dimensional O(3) nonlinear sigma model on the lattice for imaginary values of the vacuum angle ϑ.

Let us first explain why such a problem is interesting. In a euclidean metric, the partition function Z of the model in the continuum formulation is given by

$$Z = \int D[\boldsymbol{n}]\, \mathrm{e}^{-((1/f)S + i\vartheta Q)}, \tag{1}$$

where the continuum action is

$$S = \tfrac{1}{2}\int \mathrm{d}^2x\, \partial_\mu \boldsymbol{n}\, \partial_\mu \boldsymbol{n}, \tag{2}$$

and the topological charge is

$$Q = \frac{1}{8\pi}\int \mathrm{d}^2x\, \varepsilon_{\mu\nu}\, \partial_\mu \boldsymbol{n} \cdot (\partial_\nu \boldsymbol{n} \wedge \boldsymbol{n}). \tag{3}$$

* On leave from S.Ph.T. Saclay (France).

The exponent in eq. (1) may be rewritten as

$$\frac{1}{f}S + i\vartheta Q = \beta_+ \Phi_+ + \beta_- \Phi_- , \tag{4}$$

with

$$\beta_\pm = \frac{1}{f} \pm i\frac{\vartheta}{4\pi} , \tag{5}$$

$$\Phi_\pm = \tfrac{1}{2}(S \pm 4\pi Q) .$$

In the limit

$$f \to 0 , \qquad \vartheta \to \pm i\infty , \tag{6a}$$

such that

$$\beta_\pm = \ln z = \text{const} , \tag{6b}$$

the vacuum state is made of configurations for which $\Phi_\mp = 0$. This limit, after including one-loop corrections [4, 5], can be called a "semi-classical limit" because the vacuum retains only self (anti-self) dual configurations plus the contributions from quadratic (one-loop) fluctuations around these solutions. z acts like a fugacity of topological excitations controlling the density of instantons.

There has been considerable analytic study of such instanton gasses in the continuum formulation [6–8]. One knows from these studies that the instanton gas is infrared finite, generates a mass gap dynamically and is equivalent to the two-dimensional classical Coulomb gas as its critical temperature. The instanton gas is dense because the density of the Coulomb gas diverges at its critical temperature if the mass gap is held fixed.

One of the questions of interest is whether or not it is possible to construct such a semi-classical vacuum starting from a theory regularized nonperturbatively (for instance on the lattice). Another question is whether the "semi-classical limit" discussed above is analytically connected to the usual continuum limit $f \to 0$, $\vartheta = 0$*.

We shall investigate these questions by a numerical simulation of the O(3) model on a lattice at imaginary ϑ. We begin by writing down the lattice O(3) model and discuss some relevant information about the numerical simulation.

The model is defined on a square lattice on a two-torus. i denotes the sites of the lattice and $\mu = 1, 2$ denotes the two directions. At each site i a field $\boldsymbol{n}(i)$ is attached

* Let us emphasize that these considerations make sense only in euclidean space. In Minkowsky space, an imaginary ϑ violates hermiticity and positivity of the hamiltonian.

which satisfies

$$\boldsymbol{n}^2 = \sum_{a=1}^{3} n_a^2 = 1 . \tag{7}$$

The standard lattice action is

$$S = \sum_{i\mu} [1 - \boldsymbol{n}(i)\boldsymbol{n}(i+\mu)] . \tag{8}$$

We shall use for Q the definition of Berg and Lüscher [1], which gives an integer for all values of the lattice spacing a and which also connects smoothly with the continuum definition as $a \to 0$. This definition is implemented [9] in the simulation as follows:

First, divide the lattice into oriented triangles, the sum of whose areas equals the lattice area. This is done by bisecting each plaquette along a diagonal. The lattice fields $\boldsymbol{n}(i)$ on the vertices of each of these triangles define two spherical triangles on S^2. Pick the triangle σ_1 with the smaller area on S^2. This is always possible apart from 'exceptional' configurations (where the mapped triangle is a great circle). Find the oriented (spherical) area of σ_1. Q is then given by the sum of these areas over all lattice triangles divided by the area of S^2 (4π). The Q one obtains in this way is obviously an integer even if a is not zero.

In numerical simulations, it is advantageous to use the definition given above but modify slightly the method to find Q [2,9]. Instead of summing over the oriented areas of the spherical triangles, one does the following: one picks a reference point P on S^2 and determines whether σ_1 includes P or not. If it does, the contribution of σ_1 to Q is ± 1 depending on whether the mapping preserves the orientation or reverses it. The sum of such contributions over all lattice triangles is the topological charge Q.

For a numerical study, the i in eq. (1) is extremely inconvenient when $\mathrm{Re}\,\vartheta$ is nonzero. In that case, one has to use rather indirect methods [10,11] to study the theory numerically. However, when $\vartheta = i\vartheta_i$ is purely imaginary, the partition function becomes

$$Z(\vartheta_i, \beta) = \int D[\boldsymbol{n}]\, \mathrm{e}^{-(\beta S - \vartheta_i Q)} . \tag{9}$$

The integrand in eq. (9) is positive definite and one can use standard Monte Carlo methods [12] to simulate the system at any value of β and ϑ_i. Further, as the method we use to measure Q is local, each time a site spin is updated, the change in Q can be computed by a local calculation. This fact makes it possible to write fast simulation algorithms.

The order parameters we shall use to study the phases of the theory are the topological density ρ, the action per site E and the topological susceptibility χ. They are defined as follows:

$$\rho = \frac{\langle Q \rangle}{N_s} = \frac{\partial F}{\partial \vartheta_i}, \tag{10}$$

where N_s is the number of sites on the lattice and $F = (1/N_s)\ln Z$ is the free energy per site,

$$E = \langle \boldsymbol{n}(i)\boldsymbol{n}(i+\mu) \rangle = 1 + \frac{1}{2}\frac{\partial F}{\partial \beta}, \tag{11}$$

$$\chi = \frac{\langle Q^2 \rangle - \langle Q \rangle^2}{N_s}. \tag{12}$$

The rest of the paper is organized as follows: in sect. 2 we present the results of our numerical simulation with the action of eq. (8). We find a line of first-order phase transitions starting at $\beta = \infty$, $\vartheta_i = \infty$ and ending at a critical endpoint. In sect. 3 we discuss some simple instanton models in order to understand the dynamics of the phase diagram we observed. We find that the phase transition is associated with the condensation of small sized topological excitations. Since the semi-classical limit of eq. (6) cannot be achieved with the action of eq. (8), in sect. 4 we study the effects of changing the lattice action. We add a term to eq. (8) which increases the action of small sized excitations without affecting the continuum limit. With this new action, we find that for fixed β, the condensation occurs for larger values of ϑ_i. However, this increase in the critical value of ϑ_i is insufficient to reach the "semi-classical" vacuum. This section ends with our conclusions.

2. The phase diagram with the standard action. Numerical results

In this section we present the results of the Monte Carlo simulation with the simple nearest-neighbor action of eq. (8). Fig. 1 shows a hysteresis cycle for the topological density ρ as a function of ϑ_i at $\beta = 2.4$ on a 10^2 lattice. The solid and dotted lines correspond respectively to decreasing and increasing values of ϑ_i. There is a marked transition from a phase with small ρ to one with large ρ. The strong hysteresis effect indicates that this transition is of first order. For very large values of ϑ_i the density saturates at $\rho = 0.5$*.

* With the definition of ref. [1] for the topological charge, we can prove an absolute but not optimal bound of $p < \frac{2}{3}$. However, from analytic evaluation and numerical simulation, it seems very plausible that there are very few configurations with $\rho > \frac{1}{2}$. This supports the intuitive argument that in order to triangulate the two sphere S^2 once without using exceptional spherical triangles, one needs at least four triangles, leading to the bound $\rho \leqslant \frac{1}{2}$.

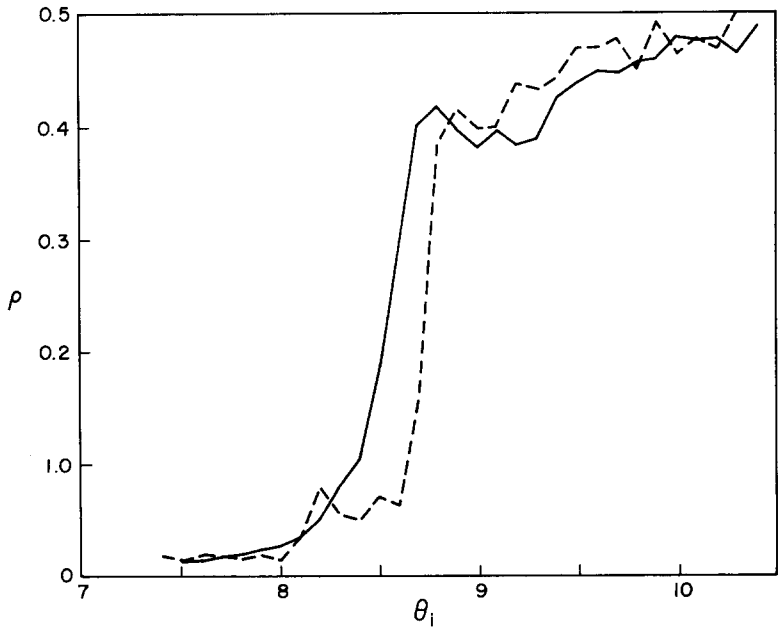

Fig. 1. Hysteresis cycle at $\beta = 2.4$ on a 10^2 lattice. The solid line represents decreasing values of ϑ_i from a dense start ($\rho = \frac{1}{2}$) at $\vartheta_i = 10.5$. The dashed line is data for ϑ_i increasing from $\vartheta_i = 7.4$ starting at $\rho = 0$. 500 iterations were discarded at each ϑ_i and 2000 were used to compute ρ. The increment in ϑ_i between measurements was $\Delta\vartheta_i = \pm 0.1$.

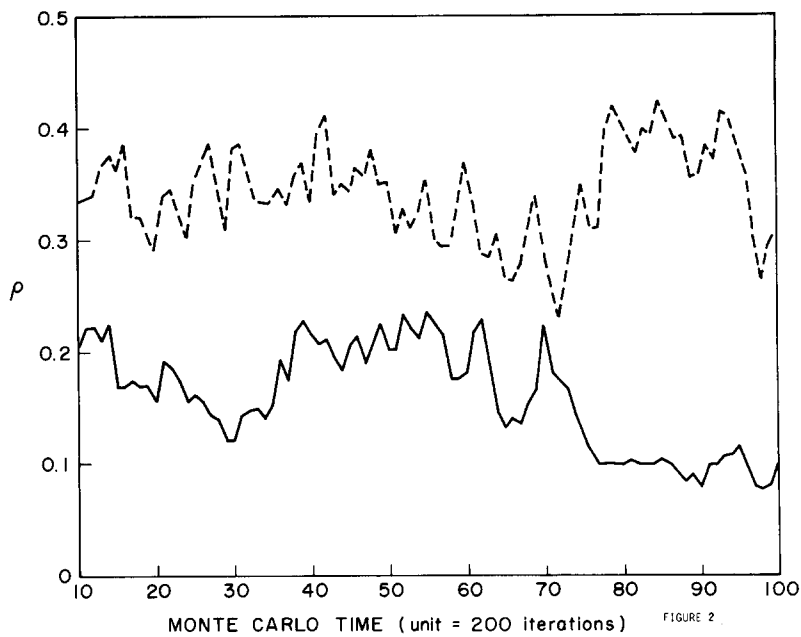

Fig. 2. Evolution of ρ at the critical point $\beta = 2.4$, $\vartheta_i = 8.7$ of fig. 1 on a 20^2 lattice. The solid (dashed) curve corresponds to an initial lattice with $\rho = 0, \frac{1}{2}$ respectively.

Fig. 2 shows the evolution of ρ from an initial configuration with $\rho = 0$ and $\rho = 0.5$ at the critical point $\beta = 2.4$, $\vartheta_i = 8.7$ as a function of simulation time. The two stable phases are clearly visible and one can estimate from fig. 2 the discontinuity L_ρ (the latent topological density) at criticality. It should be mentioned that the first-order transition also shows up at the same (β, ϑ_i) values if the average action E (see eq. (11)) is used as the order parameter.

We have studied the whole phase diagram of the theory in the (β, ϑ_i) plane by performing similar simulations at different values of β. The lattice sizes ranged from 6^2 to 20^2. The phase diagram is shown in fig. 3. The solid curve represents first-order transitions. These were located by hysteresis cycles like the one in fig. 1, where the couplings are slowly varied across the transition and the order parameters are measured. The line of first-order transitions ends at $\beta = 1.8 \pm 0.1$, $\vartheta_i = 6.8 \pm 0.2$, where the discontinuity L_ρ in ρ vanishes. The dotted line in Fig. 3 is a remnant of the first-order line. Across this dotted line, the order parameters show a marked structure but not a discontinuity. This might reflect a higher-order singularity. However, our simulation is not sensitive enough to decide this issue.

It is obviously important to study what happens to the phase diagram when the lattice size is increased. It was checked that for lattices of size up to 20^2, as long as (β, ϑ_i) are far from the critical endpoint, neither the position of the first-order transitions nor L_ρ is very sensitive to changing the lattice size. This shows that the results obtained here are not artifacts of the finite lattice sizes used.

To study the endpoint further, a detailed simulation was done at $\beta = 1.8$ on a 6^2 lattice. The results are given in fig. 4. The critical point is easily located as the position of the peak in χ. The data points in fig. 4, away from the critical region, are averages over 30 000 measurements. In the critical region ($\vartheta_i \sim [5.7, 7.5]$), they represent 125 000 measurements for each data point. Notice that even on this small lattice, although the density ρ is smooth in the critical region, χ shows a very

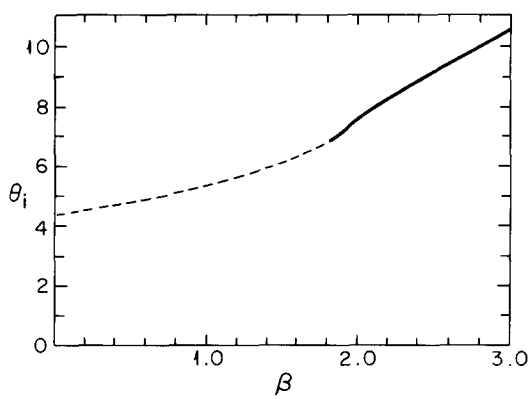

Fig. 3. The phase diagram in the (β, ϑ_i) plane. The solid line denotes first-order transition points. The dashed line locates points across which the order parameters show marked structure.

marked structure at the critical point. We have also plotted "higher-order" order parameters

$$Q_{13} = \frac{\langle Q \rangle - \langle Q^3 \rangle_c}{N_s}, \tag{13}$$

$$Q_{24} = \frac{\langle Q^2 \rangle_c - \langle Q^4 \rangle_c}{N_s}, \tag{14}$$

which are sensitive only to configurations of topological charge greater than unity. These also show a marked structure in the critical region. Although one would like to increase the lattice size to study the endpoint further, there is an additional problem related to our method of measuring the topological density. Normally, if the order parameter is a local object like E (eq. (11)) or some other spin-spin correlation function, then each configuration gives better statistics if the lattice size is increased. This is because a single configuration gives several measurements of the order parameter. However, since we only measure the total topological charge, each configuration gives a single number. Thus, increasing the lattice size only reduces the speed of the simulation. It was for this reason that the simulation at the endpoint was done on a relatively small lattice.

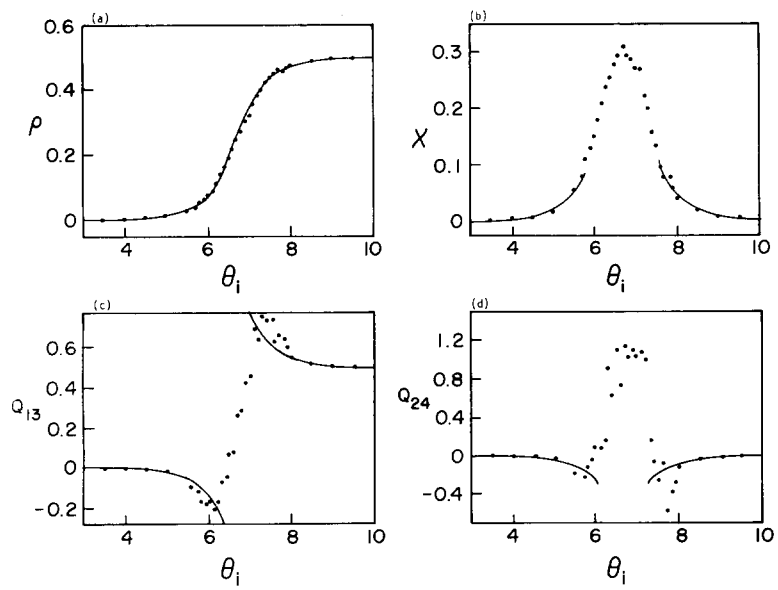

Fig. 4. Detailed study of ρ, χ, Q_{13} and Q_{24} at $\beta = 1.8$ on a 6^2 lattice. In the critical region, each point represents an average over 125 000 lattice configurations. The critical point is identified at $\vartheta_i = 6.8$. Using this, the solid curves show the results of the non-interacting instanton model (model A) discussed in the text.

It is clear that these transitions are due to the "condensation" of some topological configurations. In order to understand the mechanism of this condensation, we shall discuss in the next sections two simple analytic models which are successful in reproducing several aspects of our simulation.

3. Simple models for the phase diagram

3.1. MODEL A: NON-INTERACTING INSTANTONS

It is easy to construct a simple model which has a first-order line and a critical endpoint as in fig. 3. Let us assume that the physics is dominated by some kind of "topological excitations" (which we shall call instantons in the following). Define

$$\tilde{Z}(\vartheta_i, \beta) = \frac{Z(\vartheta_i, \beta)}{Z(0, \beta)} = \mathrm{e}^{N_s \tilde{F}(\vartheta_i, \beta)}. \tag{15}$$

For ϑ_i small (we shall call this the dilute phase), let us assume that we need an action E_0 to create an instanton from the perturbative vacuum (all spins $\boldsymbol{n}$ pointing in the same direction). Neglecting the interaction between instantons and expanding $\tilde{Z}$ around this vacuum we get

$$\tilde{Z} = 1 + \tfrac{1}{2} N_s c_1 \mathrm{e}^{-\beta E_0}(\mathrm{e}^{\vartheta_i} - 1) + \mathrm{O}(\mathrm{e}^{-2E_0\beta}), \tag{16}$$

$$\tilde{F}(\vartheta_i, \beta) = \tfrac{1}{2} c_1 \mathrm{e}^{-E_0\beta}(\mathrm{e}^{\vartheta_i} - 1) \quad \text{for} \quad E_0\beta \gg \vartheta_i. \tag{17}$$

c_1 is a factor of order unity which takes into account the number of internal degrees of freedom of the instanton.

For ϑ_i large (dense phase), let us assume that the vacuum is a condensate of instantons with density $\rho = \frac{1}{2}$. Let E_1 be the action obtained by removing one instanton from this vacuum. Note that E_1 is positive if instanton interactions are neglected. Expanding $\tilde{Z}$ around $\rho = \frac{1}{2}$ gives

$$\tilde{F}(\vartheta_i, \beta) = \tfrac{1}{2}\vartheta_i + \tfrac{1}{2} d_1 \mathrm{e}^{E_1\beta - \vartheta_i} \quad \text{for} \quad E_1\beta \ll \vartheta_i. \tag{18}$$

The factor d_1 has the same origin as c_1 and is also of order unity.

Notice that for fixed β, the free energy increases exponentially with ϑ_i in the dilute phase. In the dense phase, it approaches $\frac{1}{2}\vartheta_i$ with corrections which are $\mathrm{O}(\mathrm{e}^{-\vartheta_i})$. To minimize the free energy, the theory will switch from the dilute to the dense phase when ϑ_i becomes large enough. To locate where this happens, consider the topological density ρ:

$$\rho = \begin{cases} \tfrac{1}{2} c_1 \mathrm{e}^{-E_0\beta + \vartheta_i}, & \vartheta_i \ \text{small} \\ \tfrac{1}{2} - \tfrac{1}{2} d_1 \mathrm{e}^{E_d\beta - \vartheta_i}, & \vartheta_i \ \text{large}. \end{cases} \tag{19}$$

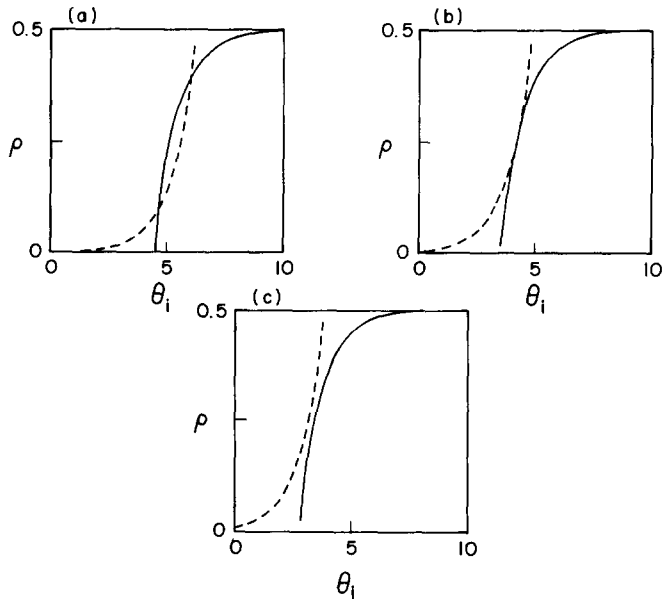

Fig. 5. The generic form of the topological density in model A (see eq. (19)). The parameters in eq. 19 have been chosen to be: $c_1 = d_1 = 1$, $E_0 = 3.5$ and $E_d = 2.5$. The β values for the three plots are respectively, $\ln 6$, $\ln 4$ and $\ln 3$. The solid line shows ρ in the dense phase and the dotted line in the dilute phase. Depending on whether the topological density ρ looks like figs. 7a, 7b or 7c, one expects a first-order transition, a continuous transition or no transition at all.

The generic form of eq. (19) is shown in fig. 5. When the curves cross as in fig. 5a, one expects a first-order transition. For increasing ϑ_i, at some point between the two points in fig. 5a where the curves cross, the dilute phase will become metastable. It will lower its free energy by jumping into the dense phase by undergoing a first-order transition. If however, the situation is as in fig. 5c, there cannot be any metastability and so there will be no transition at all. Fig. 5b corresponds to the case where the metastable region shrinks to a point. It signals the end of the line of first-order transitions. An estimate of the first-order critical point (β^c, ϑ_i^c) is obtained by taking the average values of the points of crossing of fig. 5a. This gives

$$\vartheta_i^c = \tfrac{1}{2}\beta^c(E_0 + E_1) + \tfrac{1}{2}\ln\frac{d_1}{c_1}. \tag{20a}$$

Thus, even this simple approximation is able to predict a line of transitions with slope

$$\frac{\mathrm{d}\vartheta_i^c}{\mathrm{d}\beta^c} = \tfrac{1}{2}(E_0 + E_1) \geqslant 0. \tag{20b}$$

3.2. MODEL B: A ONE-TRIANGLE MODEL

Another simple approximation consists in studying the contribution ε of a single unit triangle (half a plaquette) to the free energy. Let $\boldsymbol{n}(1), \boldsymbol{n}(2), \boldsymbol{n}(3)$ be the three spins on the vertices of the triangle as shown in fig. 6. We have, using the definition of ref. [1] for Q and dropping irrelevant constants,

$$\varepsilon = \tfrac{1}{2}\beta(x+y) + \frac{\vartheta_i}{2\pi}\cos^{-1}\frac{1+x+y+z}{\sqrt{2(1+x)(1+y)(1+z)}}, \tag{21}$$

where

$$\begin{aligned} x &= \boldsymbol{n}(1)\cdot\boldsymbol{n}(2), \\ y &= \boldsymbol{n}(2)\cdot\boldsymbol{n}(3), \\ z &= \boldsymbol{n}(3)\cdot\boldsymbol{n}(1). \end{aligned} \tag{22}$$

In this simple model, the vacuum configuration is the one that maximizes ε as a function of x, y, z. The model becomes exact in the limit $\beta \to \infty$, β/ϑ_i fixed. Extremizing ε, a simple calculation gives,

$$\begin{aligned} z &= 2x - 1, \\ y &= x, \\ \varepsilon(x) &= \beta x + \frac{\vartheta_i}{2\pi}\cos^{-1}\left[\frac{2\sqrt{x}}{1+x}\right]. \end{aligned} \tag{23}$$

Noting that x, y, z are bounded to lie in $[-1, 1]$, ε is maximum when

$$x = \begin{cases} 1 & \text{if} \quad \vartheta_i < 4\beta \\ 0 & \text{if} \quad \vartheta_i > 4\beta. \end{cases} \tag{24}$$

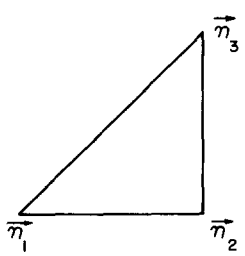

Fig. 6. The enumeration of the vertices in the one-triangle model (model B).

The point $\vartheta_i = 4\beta$ is a critical point. If $\vartheta_i < 4\beta$, the vacuum is the perturbative one: $\boldsymbol{n}(1) = \boldsymbol{n}(2) = \boldsymbol{n}(3)$. If $\vartheta_i > 4\beta$, the three-vectors are orthogonal and in the same plane: $\boldsymbol{n}(1) = (0,1,0)$, $\boldsymbol{n}(2) = (1,0,0)$, $\boldsymbol{n}(3) = (0,-1,0)$. The configuration for $\vartheta_i > 4\beta$ is clearly exceptional because the three-vectors span half a hemisphere and there is an ambiguity about which half to choose. It is also easy to see from this solution that the transition goes from $\rho = 0$ in the small ϑ_i phase to $\rho = \frac{1}{2}$ in the large ϑ_i phase. The slope $\mathrm{d}\vartheta_i^c/\mathrm{d}\beta^c$ predicted by this model is four, to be compared with the results of the numerical simulations (fig. 3), where for large β, the slope of the first-order line was close to three.

3.3. DISCUSSION

These two models give results close enough to the numerical simulation to interpret the first-order line as a condensation of small sized topological excitations which are due to exceptional configurations. The line of transitions separates a gas-like phase of instantons with small topological density from a "topological liquid" of instantons with maximum density $\rho = \frac{1}{2}$. This first-order line and its associated endpoint are reminiscent of the line of transitions separating water from water vapor in the P-T diagram of H_2O. For this reason we expect to get the corresponding Ising-like exponents at the endpoint.

To further confirm this general picture of the transition, we computed the distributions $P_1(x)$ and $P_2(z)$ of the nearest-neighbor spin product x and the diagonal spin product z (see eq. (22)) on a 20^2 lattice for ϑ_i values on either side of the transition at $\beta^c = 3.0$, $\vartheta_i^c \sim 9.5$. These are plotted in fig. 7. The solid (dashed) line corresponds to $\vartheta_i = 8$ (11) respectively. Fig. 7 clearly shows that when ϑ_i is less than the critical value, x and z are concentrated around unity signifying that the theory is in the perturbative vacuum. As ϑ_i increases beyond ϑ_i^c, configurations

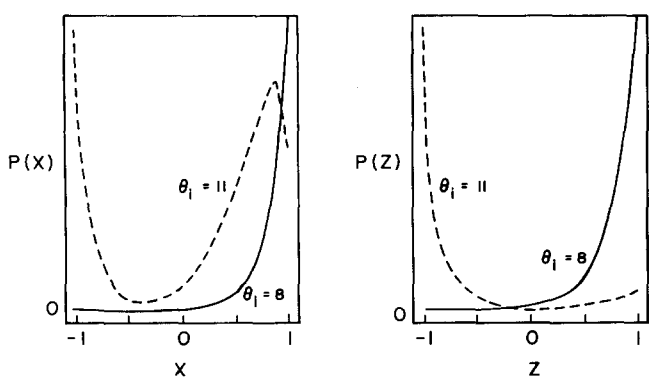

Fig. 7. The distribution of x and z (see eq. (22)) on both sides of the transition at $\beta = 3$, $\vartheta_i = 8.7$. The vertical scale is arbitrary.

where the average value of x is near 0 and z is concentrated around -1 become important. These results are in qualitative agreement with model B and show the importance of short-scale fluctuations in driving the phase transitions.

4. Results with different actions

One would like to make the contribution of the small instantons less important and try to reach the semi-classical phase near $\vartheta_i/\beta = 4\pi$ without encountering the first-order transition. To attempt this, we studied a different form for the lattice action with which one can tune a parameter δ to increase the action of "almost" exceptional configurations without changing the continuum limit. The action we used was

$$S = \sum_{i\mu} \left[1 - \boldsymbol{n}(i)\boldsymbol{n}(i+\mu) + \delta(1 - \boldsymbol{n}(i)\boldsymbol{n}(i+\mu))^2\right]. \tag{25}$$

For $\delta = 0$ one recovers the action of eq. (2) and for $\delta > 0$, the role of configurations with large topological charge is expected to decrease. In particular, in the one-triangle model discussed above, using the action of eq. (25), the transition between the "gas-like" phase and the "liquid" phase occurs, for reasonably small δ, at a value of ϑ_i given to a good approximation by

$$\frac{\vartheta_i^c}{\beta^c} = 4 + 4\delta. \tag{26}$$

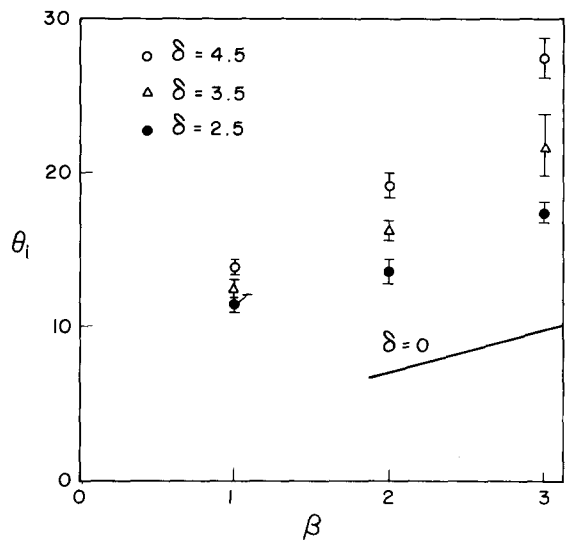

Fig. 8. Phase transitions in the (β, ϑ_i) plane for nonzero δ. The line from fig. 3 at $\delta = 0$ is also shown for comparison.

We have performed a series of simulations at different values of the parameter δ ($\delta = 2.5$, 3.5 and 4.5) and for different values of β (between 1.0 and 3.0) on a 20^2 lattice. The simulation was done from the high-density phase to the low-density phase (decreasing values of ϑ_i). We always observed an abrupt jump in ρ between the two phases, signaling a first-order transition. Fig. 8 shows the location of these transitions in the (β, ϑ_i) plane for different values of δ (compare with the results of model B, eq. (26)). Clearly, the transition occurs for larger ϑ_i as δ increases and the asymptotic slope $\mathrm{d}\vartheta_i^c/\mathrm{d}\beta^c$ for large β increases with δ. However, this increase in the slope is not sufficient to expose the "semi-classical limit" discussed before.

Fig. 9 shows the characteristics of the transitions at $\beta = 3$ in fig. 8. Figs. 9a and 9b show the density ρ and the average action E respectively as functions of ϑ_i for

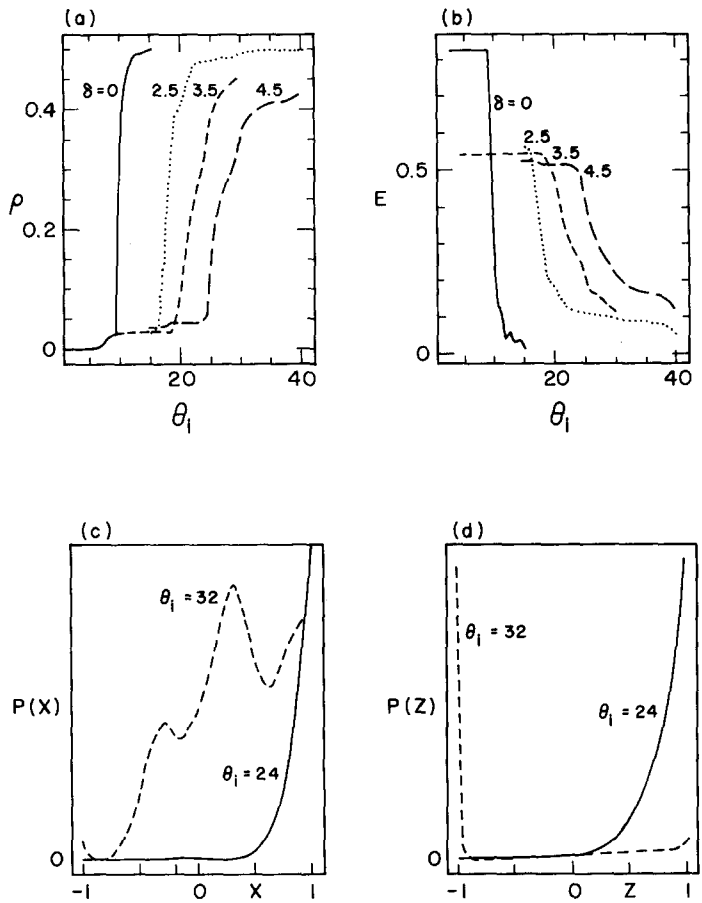

Fig. 9. (a,b) ρ and E respectively as functions of ϑ_i for $\beta = 3$ and for various values of δ. (c,d) $P_1(x)$ and $P_2(z)$ at $\delta = 4.5$ and $\beta = 3$ on either side of the transition.

various values of δ, while figs. 9c and 9d show the distributions $P_1(x)$ and $P_2(z)$ on both sides of the transition at $\delta = 4.5$ in fig. 8. This is to be compared with fig. 7 which was $\delta = 0$. Whereas these two figures differ in their details, it is clear that once ϑ_i increases beyond some critical value, configurations with x, z different from unity start to become important. This is good evidence that the transitions are caused by a condensation of small-scale topological excitations.

In conclusion, we see that when the action is modified as in eq. (25), the importance of small topological excitations decreases. However, we always find a transition due to these excitations and we have not reached a "semi-classical" regime (as defined in the introduction) where large-scale topological excitations (of a size comparable to the correlation length) dominate the physics. This is clearly related to the smallness of the instanton action in the O(3) model and the associated problems discussed in ref. [1]. It would be interesting to repeat our numerical investigation for the case of four-dimensional SU(2) gauge theories as well as higher n two-dimensional CP^n models where these problems are absent [1, 11]. In these theories, one would expect the "semi-classical" regime to be more easily accessible.

This work was supported in part by the Department of Energy under grant number AC02-76ER02220. We thank Roger Dashen, Herbert Levine and Nathan Seiberg for discussions.

References

[1] B. Berg and M. Lüscher, Nucl. Phys. B190[FS3] (1981) 412;
M. Lüscher, Nucl. Phys. B200[FS4] (1982) 61
[2] M. Lüscher, Comm. Mat. Phys. 85 (1982) 39
[3] P. Woit, Phys. Rev. Lett. **51** (1983) 638
[4] G. 't Hooft, in Proc. EPS Intern. Conf. on High energy physics, Lisbon, July 1981
[5] F. David, Phys. Lett. 138B (1984) 139
[6] B. Berg and M. Lüscher, Comm. Math. Phys. 69 (1979) 57
[7] V. A. Fateev, I.V. Frolov and A.S. Schwarz, Nucl. Phys. B154 (1979) 1
[8] A. Patrascioiu and A. Rouet, Nucl. Phys. B214 (1983) 481;
A. Rouet, Phys. Lett. 124B (1983) 379
[9] G. Bhanot, R. Dashen, H. Levine and N. Seiberg, Scaling and ϑ dependence in the O(3) σ-model, Institute for Advanced Study preprint (March 1984), Phys. Rev. Lett., to appear
[10] G. Bhanot, E. Rabinovici, N. Seiberg and P. Woit, Nucl. Phys. B230[FS10] (1984) 291
[11] G. Bhanot and N. Seiberg, Phys. Rev. D29 (Rapid Communications) (1984) 2420
[12] M. Creutz, Quarks, gluons and lattices (Cambridge University Press, Cambridge, 1984);
C. Rebbi, Lattice gauge theory and Monte Carlo simulations (World Scientific, Singapore, 1983)